Eur. Phys. J. B **3**, 211–216 (1998)

THE EUROPEAN PHYSICAL JOURNAL B

Anomalous adhesion in adsorbed polymer layers

T.J. Senden[1], J.-M. di Meglio[2,a], and P. Auroy[3]

[1] Department of Applied Mathematics, Research School of Physical Sciences and Engineering, Australian National University, Canberra, ACT 0200, Australia
[2] Institut Charles Sadron[b] and University Louis Pasteur, 6 rue Boussingault, 67083 Strasbourg Cedex, France
[3] Laboratoire de Chimie et de Physicochimie des Assemblages Supramoléculaires Organisés[c], Institut Curie, 11 rue Pierre et Marie Curie, 75231 Paris Cedex 05, France

Received: 12 November 1997 / Accepted: 6 March 1998

Abstract. Anomalous adhesion behaviour observed in the polydimethylsiloxane/heptane/silica system is reported. This behaviour is characterised by the infrequent appearance of one or more elastic minima which occur in addition to the ever-present primary adhesion. The resulting elastic force is attributed to loops connecting the tip to the substrate and can be described by two models; a worm-like chain, and a freely jointed chain. Both models give similar values for the characteristic segment length of around 0.24 nm and indicate that the chains have been extended by between 90 to 95% of their chain contour length before desorption. In some cases multiple adhesions were observed between tip and substrate and have been used to suggest a method for determining the distribution of adsorbed polymer loops.

PACS. 68.45.-v Solid-fluid interfaces – 82.70.-y Disperse systems

1 Introduction

The measurements of polymer chain characteristics such as persistence length, radius of gyration, and effective segment length are usually interpreted from bulk solution behaviour. These measurements are often highly model dependent and as they average over a large ensemble of molecules, improbable or statistically insignificant states cannot be identified. For instance, the concentration profile of an adsorbed layer of neutral polymer has been studied by neutron scattering [1] but the conformation of a single adsorbed chain was inaccessible. In order to quantify these unusual states there is a desire to directly study properties that are dependent only upon the conformation of a single chain. Recent studies on single DNA strands [2,3] elegantly demonstrated the direct elongation of a single tethered polymer chain by application of fluid flow and magnetic fields. The adhesion and stretching of biological polymers attached by specific ligand interactions has also been recently measured using force microscopy [4]. The utility of the force microscope to manipulate adsorbates and surfaces has been widely demonstrated [5–8] and is an ideal instrument for investigating the force required to extend polymer chains.

This paper draws attention to the anomalous adhesion observed in polymeric systems that may be attributable to discrete loops under mechanical strain. Although the concept of loop distribution at a polymer interface was introduced some time ago [9–11], until now it has not been directly experimentally observed.

Polydimethylsiloxane (PDMS) was chosen as the model system primarily because of its very low glass transition temperature ($T_g \simeq -120\,^{\circ}\mathrm{C}$) leading to very flexible states at room temperature, and secondly for its strong adsorption to silica [10,12]. Additionally, being a neutral polymer soluble in low dielectric solvents only short range interactions are present. This experiment illustrates the function of the force microscope in performing work on the molecular scale, and as a consequence valuable observations of discrete molecules under stress may be made. This system is very different from those studied so far by force microscopy [4] since not only the extremities adsorb, but the whole backbone is prone to adsorption *via* hydrogen bonding.

2 Experiments

2.1 Experimental system

The PDMS (α-ω trimethyl terminated) was purchased from Petrarch, subsequently fractionated by precipitation in a toluene-methanol mixture and analysed by standard GPC methods ($M_w = 221\,300$, $I_p = 1.101$). The polymer was dissolved in heptane of spectroscopic grade, purchased from Aldrich, and used as received. Heptane is known to be a very good solvent for PDMS

[a] e-mail: Jean-Marc.DiMeglio@ics.u-strasbg.fr
[b] CNRS UPR 22
[c] CNRS URA 448

having an estimated Flory interaction parameter χ_1 of 0.15 [13], giving a radius of gyration R_G of 17.0 nm [14]. Three concentrations were studied, 0.1%, 1.0% and 10%[1], covering the dilute and semi-dilute regimes. The overlap concentration c^* can be estimated to be around 0.6% [15]. For 10% solutions the average distance ξ between entanglements is about 2.0 nm [15].

Silicon wafers were oxidised [16] and had a roughness of less than 2−3 nm (r.m.s.) as measured by force microscopy. Both the cantilever and silicon wafers were cleaned by a water plasma method [16] which gave clean surfaces without change in roughness that were perfectly wet by milli-Q water. Water plasma treatment also increases the degree of surface hydroxylation, thus promoting a strong H-bonding mediated adhesion between the PDMS and silica.

2.2 Experimental technique

A Digital Instruments Nanoscope III force microscope was employed using the standard fluid cell provided. However, the usual silicone o-ring was replaced with a *C-shape* sectioned fluorosilicone o-ring. All remaining fittings were comprised of Teflon, kel-F or pyrex. Cantilevers (Digital Instruments) were calibrated via a gravimetric method [17] and considered to be silicon-rich silicon nitride [18]. The increased refractive index of the polymer solution necessitated the use of a second mirror to redirect the laser light reflected off the cantilever. Subsequently the measured signal was electronically inverted in order to maintain the initial feedback condition used to bring the surfaces into *contact*[2]. The compliance regime required to normalise the deflection-displacement curves to yield force-separation curves was found to be linear within the range of extension of the piezoelectric transducer.

2.3 Experimental procedure

In general, an approach and separation cycle was performed in ambient air, with the observation of a large adhesion due to capillary condensation between the two hydrophilic surfaces. With the injection of pure heptane an extremely large adhesion was then observed, presumably due to contact electrification [19]. This provided a qualification of the surface cleanliness of the system. After replacing the heptane with the polymer solution an equilibration period of at least several hours followed. The sharpness of the primary adhesion was used as a guide to the status of adsorption at the surface. Solvent evaporation from the cell was slow but appeared significant after a 24 hour period. The viscosity of the solution could be monitored by the amount of hysteresis, at a given speed, in the approach and separation curves recorded several microns away from contact. This was a fairly sensitive indicator of solvent evaporation for the 10% solutions.

3 Results

After the equilibration period the interaction between tip and wafer in the polymer solution, at each of the three concentrations, was featureless upon approach up until the last 5-10 nm before contact. In this range a small attraction was observed in the equilibrated systems. The range of this attraction varied from tip to tip indicating a dependence on local geometry. Within a single experiment, with the same tip, the range could be observed to increase very slightly, around 40%, by increasing the concentration from 0.1% to 10%. When the gradient of this attraction exceeded the spring constant the surfaces jumped into a position defined as *contact*. Under this initial load (< 0.2 nN) the surface could sometimes be seen to compress by around 0.4 nm, from this point onwards the surface would not yield further within the maximum load available to the instrument, *i.e.* about 10 nN. On separation the surfaces initially adhered (primary adhesion) until the gradient of the force again exceeded the spring constant and the surfaces jumped apart to a separation of 10-20 nm. Again this magnitude of this primary adhesion seems more dependent on the tip used than the solution concentration. Within a single experiment, using the same tip, the adhesion did not appear to be concentration dependent. Beyond the adhesive separation of the surfaces

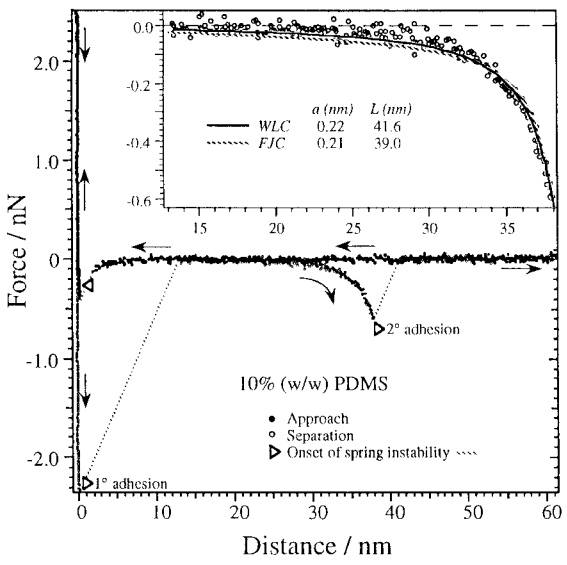

Fig. 1. An atypical approach and separation cycle for a silica surface interacting with a silicon nitride tip in a 10% (w/w) PDMS in heptane showing a secondary adhesion. The inset show the separation curve only between the two regions of zero force. The solid curve is a non-linear least-squares best fit of a worm-like chain model, dashed curve shows a freely jointed chain model. All data collected within the spring instabilities represent non-equilibrium measurements and have been omitted from the data set.

[1] All concentrations are weight/weight.

[2] The AFM technique cannot provide with an absolute measurement of the separation between tip and substrate.

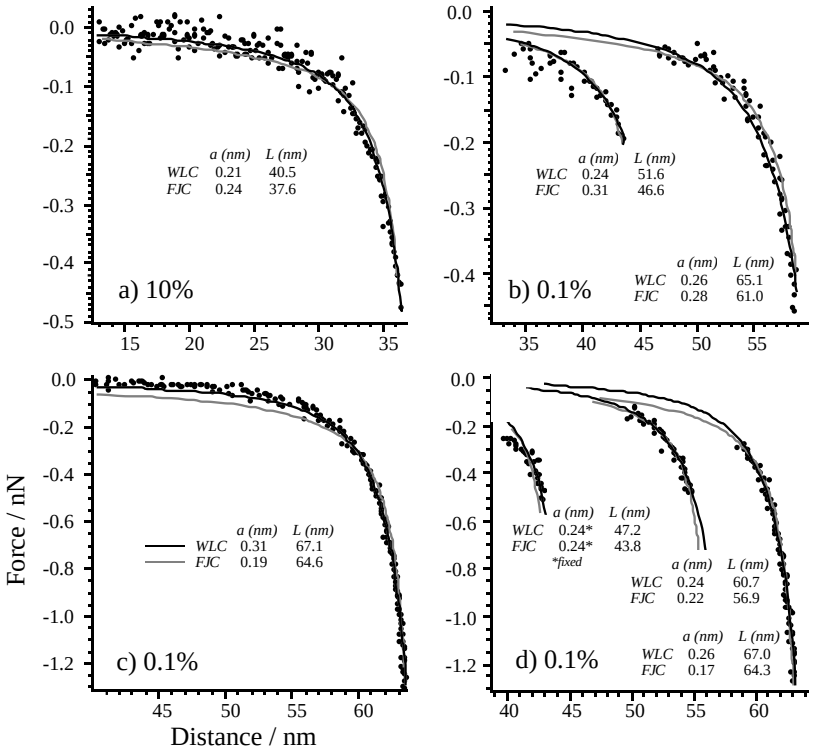

Fig. 2. A series of separations observed under different solution conditions. (a) single secondary adhesion, surfaces separate completely; (b) an additional adhesion within the secondary adhesion, surface separated completely; (c) single secondary adhesion, surfaces remained connected; (d) two additional adhesions within the secondary adhesion, surfaces remained connected.

the interaction returned to featureless at large distances. Typically the surfaces would undergo repeated approach-separation cycles with a frequency ranging from 0.1 to 10 Hz. At rates greater than 1 Hz hydrodynamic forces in the 10% solution became appreciable. This sequence of features, a small attraction followed by a moderate adhesion, within a cycle is characteristic of around 95% of interactions in the polymer solutions examined.

Upon flushing of the polymer solutions with the pure solvent the short range attraction was replaced by a repulsion which was just discernible above the background noise. The primary adhesion remained of about the same magnitude. Again this cycle is representative of around 95% of interactions in the pure solvent. This demonstrates the high affinity PDMS has for silica surfaces.

Figure 1 shows an approach and separation cycle in a 10% PDMS solution in heptane which is representative of 5% of interaction cycles exhibiting unusual multiple adhesions. On approach the surfaces met a short range attractive force at a separation of about 8 nm. On separation the surfaces initially adhered (primary adhesion) jumping apart to a separation of 13 nm. From this point the cantilever shows the same relative deflection value as at large separations, and can be said to be undeflected within the error of the measurement (*zero deflection*). On increasing the separation the surfaces begin to experience another adhesion with a non-linear dependence on distance, which ends in a spring instability at a distance of 38 nm. No repulsive interactions were observed in this system. Chain repulsion effects should not be expected to dominate interactions in the dilute to semi-dilute regimes, in which the experiments were conducted.

The extent and magnitude of the secondary adhesion seemed to be independent of polymer concentration (0.1−10%) and the cycle frequency (0.1−5 Hz). Also independent of concentration and cycle frequency was the distance of secondary adhesion minima from *contact*, which was commonly within the range 35 to 42 nm. The appearance of this secondary adhesion seemed metastable, and once present might repeat its general form on an average of 2 to 20 consecutive cycles. To some degree the secondary adhesion could be induced by leaving the surfaces in contact for a few seconds and then separating. However, this action only tended to increase the initial frequency of occurrence, and over a period of 10 seconds or so the natural frequency returned to approximately 5% of cycles.

Figure 2 shows a series of interactions observed under different solution conditions. In addition to the secondary adhesion occasionally observed, representative examples of interactions exhibiting multiple adhesions are shown. Their appearance and form also seem independent of the presence of the more usual secondary adhesion. This figure also demonstrates the condition where the surfaces are not extended beyond their point of disconnection. In this case (Figs. 2c and 2d) the surfaces remain connected and the approach curve simply shows the non-hysteretic relaxation of the tensioned chain. The attractive jump into contact and primary adhesion remained the only hysteretic component of the approach-separation cycle. Figure 3 shows a time-series of the condition where the surfaces were not separated beyond the limit of the secondary adhesion over a period of 69 seconds. During the course of this sequence the surfaces drifted apart reducing the overall load in contact by about 15%. Within many cycles additional adhesions were seen, these did not seem to effect the profile or magnitude of the secondary adhesion. Beyond this time the surfaces reverted to the occasional secondary adhesive minimum.

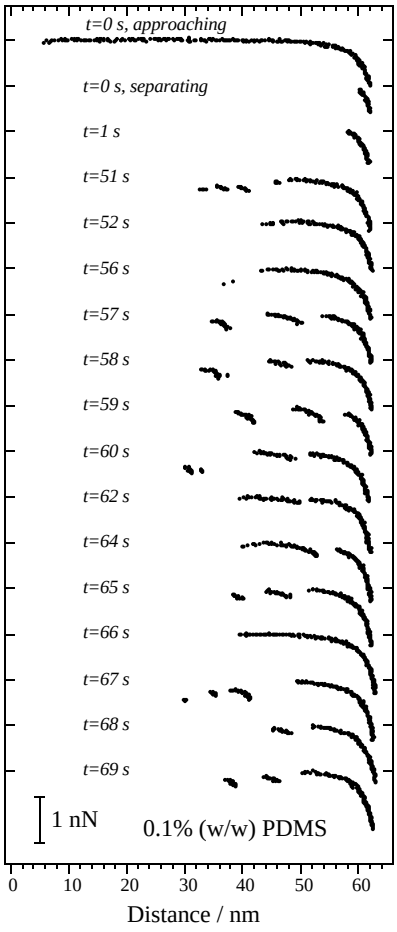

Fig. 3. A time series of cycles in which the surfaces retain the connective bridge. As the approach part of the cycle is invariant throughout the series this is shown only once, the remaining data show only separation curves. Shaded lines show regions of spring instability.

4 Discussion

As a standard imaging tip was employed, the actual area of contact was likely to be in the order of several square nanometres. This follows from the tip's ability to resolve molecular detail, for example the periodicity in silicate lattice on the surface of mica, 0.52 nm. For long range interactions an effective radius of curvature may be determined for tips. Commonly this is in the range of several hundred nanometres, and hence a contact area might be expected to be tens of nm^2 [16]. However, in this particular system interactions are short range and so the long range effective radius is a poor approximation and small scale roughness over the tip surface is the dominant geometry. The irregular nature of the contact zone does not permit the fitting of any short range interaction (*e.g.* van der Waals, depletion, *etc...*) with any certainty. The Hamaker constant of this system is likely to be low, probably less than 2×10^{-20} J [18].

The choice of surfaces and of polymer means that the most likely configuration of surface adsorbed polymer is a series of loops of randomly varying length, strongly adsorbed to the surface [10,12]. The fact the primary adhesion remains roughly constant irrespective of concentration, or presence of dissolved polymer indicates that the status of adsorption is similar in all cases. As the polymers are long (degree of polymerisation $\simeq$ 3000) there is a very low proportion of free ends and so it can be assumed that the surface is covered predominantly by loops. Figure 4 proposes the result of two polymer bearing surfaces approaching to the point of overlap between the adsorbed polymer layers. There exists then the possibility for a chain to migrate through the opposing adsorbed layer and to bridge the surfaces. The tip may well be in contact with many hundreds of loops upon each approach but it is considered a rare event for any given loop to bridge the two surfaces within the time of contact. During an average approach the surfaces may spend around a few hundred milliseconds in this regime of overlap. The possibility that secondary adhesion represents the result of an ensemble of chains bridging the surfaces can be discounted in several ways. Firstly, the adhesion profile would show no separation of the primary and secondary adhesions, there would be a single adhesion event. As the profile would be due to a collection of chains in many possible states one would expect little variation in the profile with each separation, and expect to see this adhesion phenomena on every separation cycle. The final release of the two surfaces would be a continuous process and not a sudden step process as observed. Finally, the single adhesion profile would follow an exponential decay law, which is clearly not the case.

Once a connective bridge is formed it may be strained normal to the surface until a yield point is reached. This point of yield might have two possible causes: chain scission, or desorption when the elastic energy of the chain exceeds the adsorption energy. In the first situation the magnitude of the measured force is slightly below the range reported for bond scission of a C-C bond, *i.e.* 2.6−13.4 nN [20] or 4−6 nN [21]. However, as the Si-O bond has a bond enthalpy some 30% higher [22] than the C-C bond so one might expect the Si-O bond to be more resistant to scission. As the forces at separation are found to be in the range of a few tenths of a nN to around 2 nN it is more likely that the magnitude of the adhesion reflects the nature of the PDMS-substrate interaction. The strength of this interaction is due to hydrogen bonding between the surface silanols and the silyl ethers of the PDMS backbone. The strength of numerous hydrogen bonds acting in a concerted manner should not be underestimated. The remarkable bond formed between the association of streptavidin and biotin is a result of only four direct hydrogen bonds and four bridging water molecules [23].

Modelling the force law of chain elongation may be approached easily in two ways, treating the loop as a Freely Jointed Chain (FJC) [2,24,25] or as a Worm-Like Chain (WLC) [3,26]. A freely jointed chain is comprised of independent, unaligned segments of length a (Kuhn length). Each segment can be thought of a dipole and by application of an electric field these dipoles may be aligned. The elasticity of the chain comes from the entropic tendency

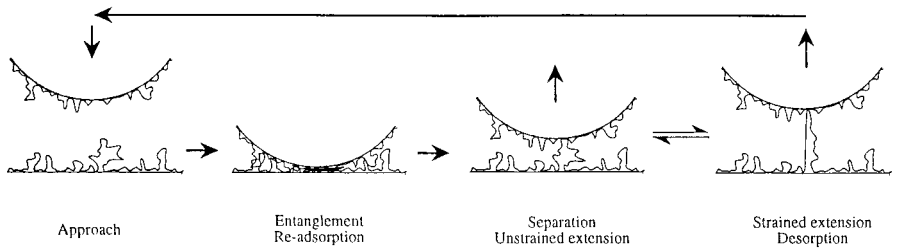

Fig. 4. A scheme showing a possible path to the formation and extension of a connective bridge.

to disorder the segments. The average end-to-end distance x of such a chain with contour length L influenced only by thermal energy kT and an external force F can be described by the Langevin equation:

$$x = Na\left(\coth\frac{Fa}{kT} - \frac{Fa}{kT}\right) \tag{1}$$

where the number of segments N is given by L/a.

In a worm-like chain the elasticity is determined by a persistence length b. The system can be treated quantum mechanically and Bustamante [3] summarised the equation for the force as a function of extension:

$$F = \frac{kT}{b}\left(\frac{1}{4}\left(1-\frac{x}{L}\right)^{-2} - \frac{1}{4} + \frac{x}{L}\right)\cdot \tag{2}$$

The choice of b is limited by the lower bound of the Si-O bond length of 0.165 nm [27] and an upper bound of around 1.0 nm determined from viscoelastic properties of PDMS chains [28]. Likewise the chain would seem highly extended from the data so L should be close to, and not lower than, the onset of the spring instability.

The two models were fitted to the data at forces greater than 0.1 nN, using a (or b) and L as fitting parameters, with attention paid to goodness of fit at high extensions. In general the WLC model fits the data over the widest range. The FJC model can be made to fit moderately well at either low extensions or at high extensions. The WLC analysis gives a value for b of 0.23 nm (std. dev. 0.02 nm for 35 samples), while a slightly higher value for a of 0.25 nm (std. dev. 0.04 nm) was obtained from the FJC analysis. These values, that are almost identical since the PDMS is highly flexible, are in good agreement with the value of 0.25 ± 0.1 nm obtained from neutron scattering data [1]. Chain extensions at the point of desorption predicted from the WLC model are on average 89% of the fitted contour length. The FJC model however predicts a higher degree of extension on average at 96% of the contour length. Note that bulk entanglements are not detailed since they should not contribute to the force. Indeed, the reptation time of individual chains can be evaluated to be around a millisecond which is a much shorter time than the characteristic time of the tip motion (1 second). The rarity of the secondary adhesion would suggest that only a single loop is withdrawn at a time, which is corroborated by the independence of the fitting parameters in the case of multiple adhesions. These experiments suggest that it might be possible to obtain the loop length distribution of the adsorbed chains by assuming that the maximum in the secondary adhesion marks a detachment distance, which is proportional to the contour length of the strained segment.

Figure 5 shows the frequency of occurrence of the detachment distances for an entire set of experiments. The analysis of the stretching of a single loop, as described above, showed that the loops are almost completely stretched when they detach from the surface. We can thus assume that the frequency of detachment distances *versus* distance is the same as the distribution of the loops with n monomers *versus* n. This distribution can be theoretically derived from the original work of de Gennes [9] on the loop distribution of a single adsorbed chain. Although this model holds only for monomer adsorption energies of the order of kT, the data may still be compared on the basis that a single hydrogen bond is around this order. This does not exclude the possibility that many hydrogen bonds acting in unison. Considering, a layer of thickness d located at a distance z from the adsorption plane;

$$\phi(z)dz = g(n)dn \tag{3}$$

where, $\phi(z)$ is the monomer volume fraction, and $g(n)$ the probability that a monomer belongs to a loop with more than n monomers. The average distance between entanglements is denoted ξ. For $z > \xi$, which corresponds to a tip substrate separation of about 4 nm (2ξ), the concentration profile $\phi(z)$ is constant. We thus get $g(n) \propto n^{-1/2}$ since $z = an^{1/2}$ for chains over distances larger than ξ.

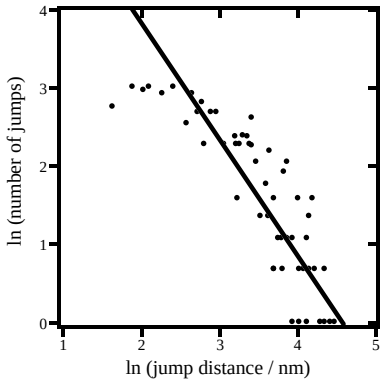

Fig. 5. Plot of the frequency of occurrence of detachment distances. The detachment distance is assumed to be proportional to the contour length, and hence the number of monomers in the extended chain (10% w/w PDMS).

The distribution $S(n)$ of loops can then be derived;

$$S(n) = -\frac{\partial g(n)}{\partial n} = n^{-3/2}. \quad (4)$$

The solid line in Figure 5 corresponds to this prediction and it is clear that the data scales similarly in the 10−100 nm range. Mean field theories [29] predict a stronger dependence of the frequency *versus* distance when $z < \xi$. This are not observed, on the contrary, it appeared that the tip did not pick up any loop smaller than 1.0 nm. Clearly the magnitude of the primary adhesion masks all loops smaller than several nanometres in length. The contour length for the molecular weight studied is around 700 nm. Hence the length of bridges rarely exceeded more than 10% of total contour length, and were commonly within the range of $2R_G$ from contact. These distances compare with a long-range radius of curvature for the tip of several hundred nanometres.

The failure to observe a depletion interaction below c^* at a surface separation around $2R_G$ might be explained in two ways. Firstly, any depletion attraction would be of low magnitude, say around several hundred $\mu\mathrm{Nm}^{-1}$ [30]. Even at the largest possible curvature for the tip of several hundred nanometres the interaction would not exceed 100 pN. Given the likely roughness of the tip this value could only be expected to be smaller. Similarly with the van der Waals interaction, the expected contribution would be in the order of tens of pN. The second possibility is that the chains adsorb very strongly resulting in bridging effects dominating any depletion interaction. As the effective short range radius of the tip is not known it is difficult estimate the distance dependency of the attractive profile. The range of the attraction does seem to increase very slightly with concentration, and comparisons within experiments employing the same tip show that range of the attraction increases by about 40% from concentrations of 0.1% to 10%. The profile does not appear to follow a power law relationship with distance, but as the local tip geometry is unknown it is premature to comment in detail on this observation.

5 Conclusion

In conclusion these experiments suggest a novel way of investigating conformational characteristics of adsorbed polymers. Through the chance bridging and subsequent elongation of a loop the distribution of loop lengths and chain persistence length can be realised. Studies on the effects of solvent quality, density of adsorption sites and polymer structure can be imagined. Systems as complex as cell surfaces might be explored simply in this manner.

This study has been initiated in the Department of Applied Mathematics in Canberra, then continued in the Laboratoire de Physique de la Matière Condensée in Paris and finalized in the Institut Charles Sadron in Strasbourg. We thank Miguel Aubouy, Hugh Brown, Pierre-Gilles de Gennes, Liliane Léger, Elie Raphaël, in Paris, Jean-François Joanny, Albert Johner, Patrick Kékicheff and Carlos Marques in Strasbourg, and David Williams in Canberra for numerous and useful discussions. TJS thanks the Collège de France for their hospitality and financial support extended during his visit. JMdM thanks the Australian National University for their hospitality; his stay in Canberra was made possible thanks to the Rhône-Poulenc Australian Fellowship in conjunction with the Australian and French Academies of Sciences and the Australia-France Foundation.

References

1. L. Auvray, J.-P. Cotton, Macromol. **20**, 202 (1987).
2. S. Smith, L. Finzi, C. Bustamante, Science **258**, 1122 (1992).
3. C. Bustamante, J.K. Marko, E.D. Siggia, S. Smith, Science **265**, 1599 (1994).
4. M. Rief, F. Oesterhelt, B. Heymann, H.E. Gaub, Science **275**, 1296 (1997).
5. C.M. Mate, Phys. Rev. Lett. **68**, 3323 (1992).
6. E. Hamada, R. Kanek, Ultramicroscopy **42-44**, 184 (1992).
7. S.O. Akari *et al.*, Appl. Phys. Lett. **65**, 1915 (1994).
8. J.-P. Aimé *et al.*, J. Appl. Phys. **76**, 754 (1994).
9. P.-G. de Gennes, C. R. Acad. Sci. Série II **294**, 1982 (1317).
10. O. Guiselin, Europhys. Lett. **17**, 225 (1992).
11. G.J. Fleer *et al.*, *Polymers at Interfaces* (Chapman & Hall, Cambridge, England, 1993), p. 31.
12. E. Bouchaud, M. Daoud, J. Phys. A. **20**, 1463 (1987).
13. A. Muramoto, Polym. J. **1**, 450 (1970).
14. A. Lapp, J. Herz, C. Strazielle, Makromolek. Chem. **186**, 1919 (1985).
15. A. Lapp, C. Picot, C. Strazielle, J. Phys. Lett. **46**, L1031 (1985).
16. C.J. Drummond, T.J. Senden, Coll. Interf. A **87**, 217 (1994).
17. T.J. Senden, W.A. Ducker, Langmuir **10**, 1003 (1994).
18. T.J. Senden, C.J. Drummond, Coll. Interf. A **94**, 29 (1995).
19. B.D. Terris, J.E. Stern, D. Rugar, H.J. Mamin, Phys. Rev. Lett. **63**, 2669 (1989).
20. J.A. Odell, A.J. Keller, Polym. Sci. B **24**, 1889 (1986).
21. T.Q. Nguyen, H.H. Kausch, Colloid Polym. Sci. **269**, 1991 (1099).
22. G.H. Aylward, T.J.V. Findlay, *S.I. Chemical Data*, 2nd ed. (Jacaranda Wiley, Brisbane, Australia, 1974), p. 101.
23. H. Grubmüller, B. Heymann, P. Tavan, Science **271**, 997 (1996).
24. W. Kuhn, E. Grün, Kolloid Z. **101**, 248 (1942).
25. H.M. James, E.J. Güth, Chem. Phys. **11**, 1943 (455).
26. M. Fixman, J.J. Kovac, Chem. Phys. **58**, 1564 (1973).
27. E.H. Aggarwal, S.H.J. Bauer, Chem. Phys. **18**, 42 (1950).
28. S.M. Aharoni, Macromol. **19**, 426 (1986).
29. A. Johner, J.-F. Joanny, M. Rubinstein, Europhys. Lett. **22**, 591 (1993).
30. P. Richetti, P. Kékicheff, Phys. Rev. Lett. **68**, 1951 (1992).